TECHNICAL AND ENVIRONMENTAL EVALUATION OF HEAT TRANSFER FLUIDS USED IN SOLAR POWER TOWERS

Gülden Adıyaman[1], İlhami Horuz[2], Levent Çolak[1]
[1]Başkent University, Faculty of Engineering, Mechanical Engineering Department, Ankara, Turkey
[2]Gazi University, Faculty of Engineering, Mechanical Engineering Department, Ankara, Turkey
Corresponding author: Gülden Adıyaman, e-mail: gulden@baskent.edu.tr

REFERENCE NO

SOLR-05

Keywords:
Solar power tower, solar receiver, heat transfer fluids, computational fluid dynamics, exergy, CO_2 emission

ABSTRACT

The solar power tower is one of the most promising technologies in concentrating solar systems for electricity generation from solar energy. Central receiver is important component of solar tower system. Because the incident radiation from the heliostats is absorbed directly by the heat transfer fluid in the receiver. In this study, Solar Two central receiver was modelled for model verification. And then, six different gases and liquid metals were carried out in ANSYS Fluent, temperature changes on the receiver and receiver thermal efficiency were obtained and discussed. The environmental impact of these fluids had been researched and examined.

1. INTRODUCTION

In the last century, the development of industry and technology has led to an increase in energy demands. Fossil fuels with limited resources and environmental problems require new sustainable electricity generation options. An important alternative for increasing energy demand is solar energy, which is one of the renewable energy sources. Electricity generation from solar energy has increased dramatically in recent years, and the use of optically concentrated solar technologies, which provide particularly high thermal power, has gained importance. The solar power tower (SPT), one of the optical condensing solar systems, is one of the most promising technologies for electricity generation from solar energy.

The SPT consists of three main subsystems: the heliostat field, central receiver and power block. In STP systems, sunlight is concentrated and reflected by heliostat field onto the receiver. For a conventional system the incident energy is then transferred from the receiver through tube walls to heat a heat transfer fluid (HTF). The HTF is then passed directly through a heat exchanger to generate steam for a Rankine cycle.

Receiver is important component of SPT system. Because the incident radiation from the heliostats is absorbed directly by the heat transfer fluid (HTF) in the receiver. Heat transfer fluids used in receivers directly affect the efficiency of solar tower systems. Today, central receivers use water and molten salts (solar salt or nitrate salt), which allow easy thermal storage. Recent studies have shown that, in addition to conventional fluids, various fluids can be used in receivers.

Computational Fluid Dynamics (CFD) software, which is used to analyse thermal efficiency in receivers, save time. In addition, temperature fluctuations on the receiver and thermal losses can be easily examined.

Colomer et al. presented a method for detailed modelling of heat transfer and flow dynamics in solar tower receivers. They have made numerical solutions by separating the receiver model into 4 sub-models as heat conduction, two-phase flow, radiation and natural convection [1]. Rodriguez-Sanchez et al. presented a thermal model for the receiver. The radiation from an external tubular receiver operating with a salt solution was modelled and receiver was drawn as a polygon in the form of flat panels. Thermal, mechanical and hydrodynamic analyses of the receiver were performed. Thermal analysis showed that radiation losses were higher than in the literature and therefore thermal

efficiency is lower [2]. Kribus et al. studied receiver designs that could be adapted to systems designed for power generation with the solar tower, and showed how temperature and power output changed [3]. Yang et al. experimentally investigated the interaction between the heat transfer performance and thermal efficiency of a receiver which used molten salt as HTF [4]. Christian and Ho used ANSYS Fluent to evaluate and characterize radiative and convective losses in the Solar Two central receiver. This study presented a model that could be used for receiver design and demonstrated whether current convective correlations were suitable for analytical evaluation of external solar tower receivers [5]. Zanino et al. investigated the effects of the Reynolds Average Navier-Stokes (RANS) type turbulence model selection available in Fluent in the case of convective thermal losses occurring in the Solar Two central receiver [6].

Pacio and Wetzel focused on the current state of liquid metal technology. Based on basic requirements and previous experience, three main liquid metals proposed; sodium (Na), lead-bismuth eutectic alloy (LBE or PbBi) and molten tin (Sn) [7]. Boerema et al. examined the utility of two heat transfer fluids, Hitec molten salt and liquid sodium in solar tower receivers. Liquid sodium; was shown as potential for solar thermal power systems due to their wide operating temperature range [8]. Bellos et al. examined the potential fluids that could be used in parabolic trough collectors in the large temperature range of 300 K to 1300 K. Examined working fluids; water, Therminol VP-1, solar salt, liquid sodium, air, carbon dioxide and helium. As a result of the study, it was proven that liquid sodium exhibits maximum exergetic efficiency (47,48%). The maximum exergetic efficiency of helium, carbon dioxide and air were 42,21%, 42,06% and 40,12%, respectively [9].

2. MODELING AND SOLUTION

2.1. Geometry and Mesh

Solar Two solar power tower receiver was the external receiver type had a roughly cylindrical shape, approximated by a polyhedron made of 24 heat absorbing panels. Each panel was composed of 32 individual tubes to transport the molten salt (Fig. 1) [10].

Fig. 1. Solar Two receiver [10]

Receiver was modelled and ANSYS Fluent 18.1 version which is CFD software was used for numerical solutions. The receiver model geometry was simplified and modelled in ANSYS Design Modeler. The receiver modelled in Fig. 2 is shown. Simplified panels are arranged as a polygon with a radius of 5,1 m. Receiver consists of 24 panels. The height of each panel is 6,2 m.

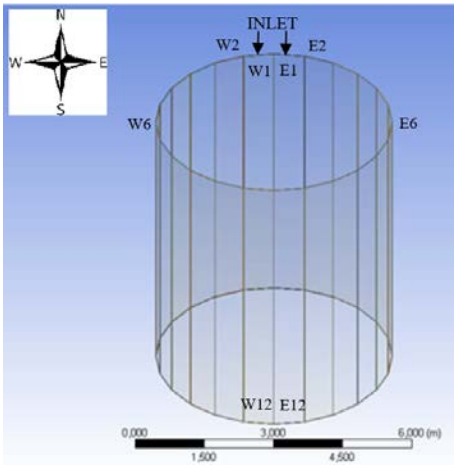

Fig. 2. Model of the Solar Two receiver with simplified absorbing panels

Only flow areas were modelled. Since the outside diameter of the panel tubes was 2,1 cm and the thickness was 1,2 mm, the flow area of the molten salt was calculated as 18,6 mm. Computational domain is a hexahedron

with a square horizontal base of 30 m width and a height of 36 m (Fig. 3).

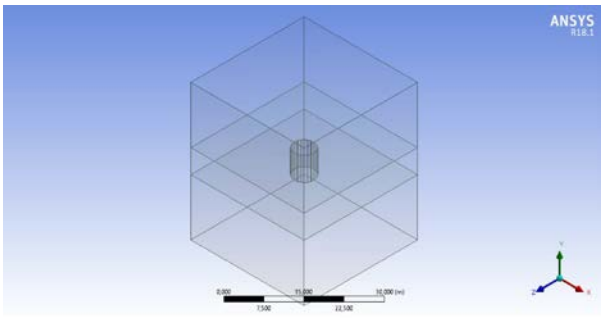

Fig. 3. Receiver and air domain model

The grid structure of the model is shown in Figure 4. More frequent mesh structure was used in the mid-region of the air domain in contact with the receiver. This is why the turbulence in that region and the heat transfer between the receiver and the air domain are calculated at high accuracy.

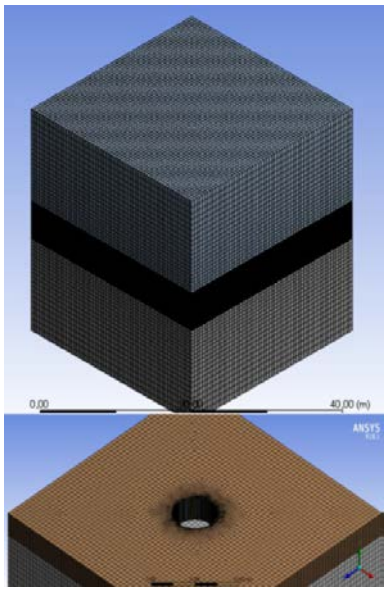

Fig. 4. Mesh structure of model (top), half section of model with mesh (bottom)

The grid structure element number is approximately 600000. The skewness of the mesh elements is 0,58. This number has been resolved in many element counts, until the independence from the mesh element number in the results, and the appropriate number of elements has been determined.

2.2. Fluent Boundary Conditions

CFD solutions were made in steady-state regime. k-ε RNG turbulence model and DO (Discrete Ordinates) radiation model were used. Figure 5 illustrates the serpentine flow arrangement between adjacent receiver panels. Molten salt enters the receiver through the two northernmost panels (panels E1 and W1), flows in a serpentine pattern through the adjacent six panels, crosses over from one side of the receiver to the other along the east-west centerline, then completes the path through the remaining six panels, exiting the receiver through panels E12 and W12. This single crossover, serpentine flow path is illustrated in Figure 5 [10].

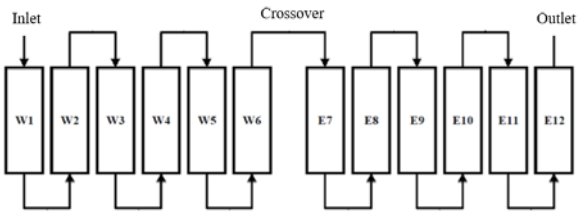

Fig. 5. Receiver Crossover Flow Pattern [10]

As seen in the simplified model of the receiver, the connection pipes between the panes were not modelled. In order to provide the flow of serpentine shown in Figure 5 without such a pipe model, a boundary condition called 'recirculation inlet-outlet' was used in Fluent. Thermal losses and pressure drops due to connection tubes were neglected.

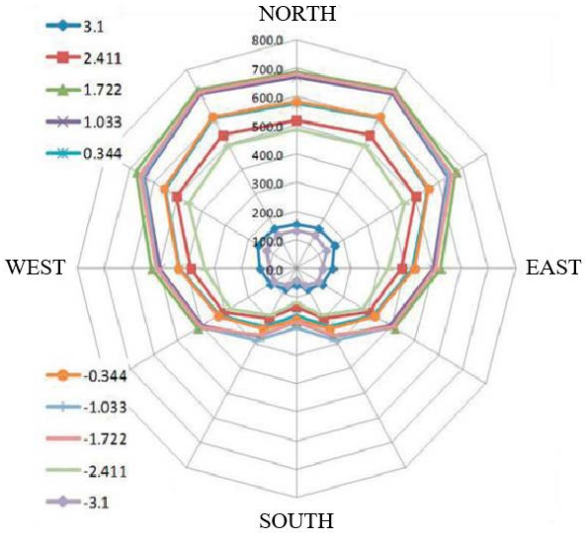

Fig. 6. Radiative load (kW/m^2) on the receiver, as a function of angular position and height along the receiver (m) [6]

The azimuthal and axial distributions of the load on the receiver are obtained by

interpolation of the map in Fig. 6, assuming a constant value on each rectangular tile. Each panel was approximated by a single channel of roughly rectangular cross section, sub-divided vertically into 10 partitions. The surface heat load (W/m^2) on the receiver computed by the DELSOL code, corresponding to a total incident power of 40 MW [6]. In Fluent, a volumetric heat load (W/m^3) was estimated and applied, dividing the surface heat load by the actual tube wall thickness 1,2 mm. On the internal surface of the receiver adiabatic conditions were assumed.

Mass flow rate of 45 kg/s of molten salt ($T_{in,ms}$ = 563 K) was flowing in each half of the receiver, and the wind was assumed to flow from the west onto the receiver at temperature $T_{in,air}$ = 300 K and speed V_{air} = 8,98 m/s.

2.3. Model Validation and Results

The study of Zanino et al. [6] was taken as a reference for verification of the model. Table 1 shows the study results and reference results. The results are in accordance with the reference study and the error rates are acceptable. The differences in the results are largely due to mistakes made in reading the values on the radiation map in Fig. 6.

Table 1. Comparison of reference results with study results

	Study	**Reference [6]**	**Error percentage (%)**
Convection loss (MW)	0,89	0,87	2,30
$T_{out,ms}$ (K)	831,77	823,50	1,00

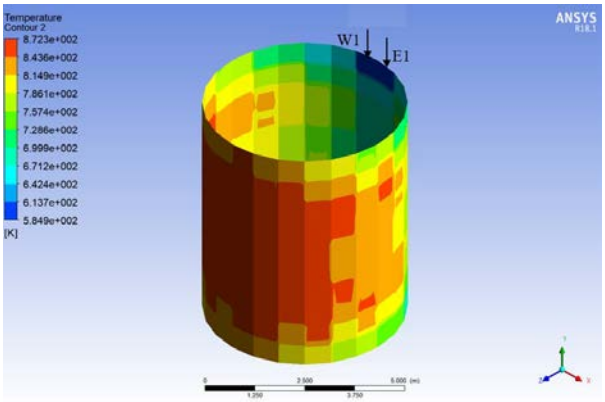

Fig. 7. Temperature distribution on the receiver

The temperature distribution on the receiver is shown in Figure 7. Although the average temperature of the receiver is 792 K, temperature distributions on the receiver reach up to 872 K. A uniform temperature distribution has not been observed due to non-uniform heat load. The values above the mean temperature were generally on the outlet panels of the molten salt.

The sum of radiation and convection losses is 2,78 MW. This loss of 1,88 MW of radiation, 0,89 MW of convective losses. As can be seen, the radiation losses are about 2 times that of the transportation losses. According to CFD results, the thermal efficiency (η_{th}) of the receiver is calculated according to Equation 1 and result is 87,67%. Conduction losses in calculations, average loss from Solar Two experiments was taken as 0,3 MW [10].

$$\eta_{th} = \frac{\alpha}{1 + \frac{Q_{loss}}{Q_{abs}}} \quad (1)$$

Where α is the reflection ratio (0,95) of the Pyromark paint on the receiver surface. Q_{abs} (W) is the power absorbed by the heat transfer fluid in the receiver, and Q_{loss} (W) is the total conduction, convection and radiation losses from the receiver to the surroundings.

$$Q_{abs} = \dot{m} c_p \left(T_{out,htf} - T_{in,htf}\right) \quad (2)$$

Where $\dot{m}$ is mass flow of HTF, and unit is kg/s. c_p is the average specific heat between HTF inlet and outlet temperature (J/kgK), $T_{in,htf}$ and $T_{out,htf}$ are the inlet and outlet temperatures of HTF in K units.

3. TECHNICAL EVALUATION

The heat transfer fluid used in the receiver affects the efficiency of the receiver. The thermophysical properties of the fluid used influence the thermal power absorbed by that fluid. This is an important parameter for receiver efficiency. Six different fluids (gas and liquid metal) were analysed in the study, which were lighted in the literature investigations. All analyses were carried out

in the Solar Two flow path at 45 kg/s and 563 K inlet temperature for E1 and W1 panels.

On the receiver used air as HTF, the thermal losses were 3,68 MW. The thermal efficiency of the receiver was 85,49%. The exit temperature of air was 929 K. The average temperature of the receiver was 859 K. The highest temperature seen on the receiver surface was 971 K, as shown in Figure 8(a). As expected, the lowest temperatures were observed in the North direction, the temperature increases in the South direction and reaches the highest value in the South side panels.

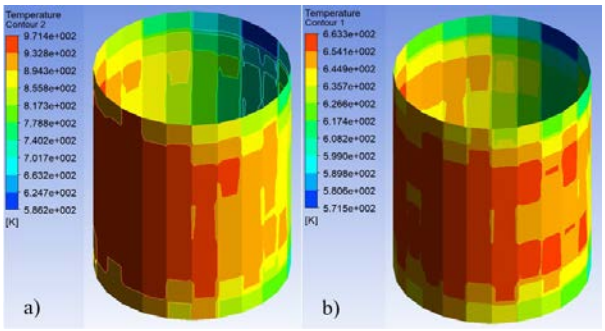

Fig. 8. Temperature distribution on the receiver using Air (a) and Helium (b)

On the receiver used Helium (He), a significant decrease in thermal losses was observed. Radiative and convective losses were only 1,38 MW. The efficiency of the receiver was 90,98%. The reason for the high efficiency was the low receiver temperature as shown in Figure 8(b). The average temperature of the receiver was 639 K, while the highest temperature was only 663 K. The outlet temperature of the He gas was 644 K.

The average receiver temperature in the receiver using Neon (Ne) gas was found to be 869 K. Figure 9(a) shows the temperature distribution of the receiver. The outlet temperature from the W12 and E12 panels of Neon gas was 947 K on average. The thermal efficiency of the receiver with a total loss of 4,14 MW was calculated as 85,12%.

The temperature distribution of the receiver using liquid Sodium (Na) is shown in Figure 9(b). When the receiving temperature was 782 K, the outlet temperature of Sodium was 884 K. The radiation losses on the receiver were 1,85 MW and the convective losses were 0,87 MW. The efficiency was calculated as 87.78%.

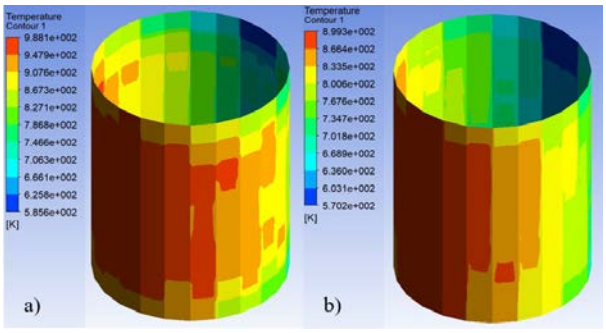

Fig. 9. Temperature distribution on the receiver using Neon (a) and Sodium (b)

In the receiver using Sodium-Potassium (NaK) eutectic, the thermal losses were 4,38 MW. The thermal efficiency was 84,58%. As seen in Figure 10(a), temperatures above 1000 K appear on the receiving surface. The average receiving temperature was 877 K.

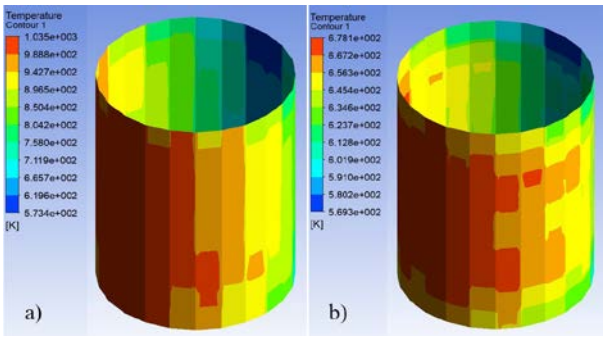

Fig. 10. Temperature distribution on the receiver using Sodium-Potassium eutectic (a) and Lithium (b)

The results obtained from the receiver using Lithium (Li) as heat transfer fluid were similar to those obtained from Helium gas. Figure 10(b) shows the temperature distribution of the receiver. The total thermal losses from the receiver with an average temperature of 644 K were 1,72 MW. In these conditions, the thermal efficiency of the receiver was calculated as 90,89%. However, the temperature of the liquid Lithium increased only in the receiver to 665 K.

The receiver thermal efficiency varied between 84,54 and 90,98%. Fluids with higher efficiency than Solar Two were Helium, Lithium and Sodium. Apart from Sodium, the panel outlet temperatures were less than the molten salt, although the thermal efficiencies

of Helium and Lithium were higher than the molten salt. Table 2 shows the average surface temperature, thermal efficiency, outlet temperature and exergetic efficiency results from HTF's.

Although the inlet temperatures are the same, Lithium and Helium with the highest thermal efficiencies were found to have the lowest outlet temperatures. On the other hand, the quality of the energy is directly related to the temperature. Since this can be explained by the exergetic efficiency (η_{ex}) which accounts for the rate of utilization of the energy, the exergetic efficiency values are calculated using Equation 3 for these fluids [11].

$$\eta_{ex} = \frac{Q_{abs}\left(1-\frac{T_{amb}}{T_{rec}}\right)}{Q_s\left[1-\frac{4}{3}\left(\frac{T_{amb}}{T_s}\right)+\frac{1}{3}\left(\frac{T_{amb}}{T_s}\right)^4\right]} \quad (3)$$

where T_s is the sun temperature (5777 K), T_a is the ambient temperature (300 K) and T_{rec} is the average surface temperature of the receiver. Q_s is the concentrated beam radiation absorbed by the absorber (40 MW).

Table 2 shows that the Sodium-Potassium fluid, which has the highest output temperature, provides the highest quality output energy.

Table 2. Results for solar receivers for different HTF's

Heat Transfer Fluids	**T_{rec} (K)**	**η_{th} (%)**	**$T_{out,htf}$ (K)**	**η_{ex} (%)**
Helium	639	90,98	644	53,97
Lithium	644	90,89	665	54,83
Sodium	782	87,78	884	60,87
Molten salt	792	87,67	832	61,27
Air	859	85,49	929	62,60
Neon	869	85,12	947	62,60
Sodium-Potassium	877	84,54	1015	63,20

Table 2 shows that although the highest thermal efficiency is obtained from Helium gas, the exergetic efficiency is the lowest among other fluids. That means the quality of energy for obtaining electricity is low for that fluid. Due to quality of energy output of solar receiver, the best result can be obtained from Sodium-Potassium which has the highest exergetic efficiency.

4. ENVIRONMENTAL EVALUATION

Fluidized bed technology is widely used in electricity generation by thermal power plants in order to obtain working fluid at high temperature. However, fossil fuels are used in these systems and CO_2 emission is also emitted accordingly.

The mass flow rate of CO_2 emission per hour of thermal systems can be calculated by the following equation:

$$\dot{m}_{CO_2} = c_i \frac{Q_{output}}{\eta} \quad (4)$$

Where c_i is the CO_2 emission amount per unit input energy that is obtained from fossil fuel combustion. η is the overall efficiency of the fluidized bed (0,88) and Q_{output} is the thermal energy obtained from the fluidized bed. When lignite is used as fuel in fluidized bed, the value of c_i for lignite is about 0,33 $kgCO_2/kWh$ [12]. In this study Q_{output} were taken as thermal power output (Q_{abs}) of solar power tower receiver where thermal power outputs and corresponding CO_2 emission decreasing amounts for different HTFs are given in Table 3.

Table 3. Decrease in CO_2 emission due to HTF used in SPT

Heat Transfer Fluids	**Thermal Power Output (MW)**	**Decrease in CO_2 emission (tonCO2/h)**
Helium	38,32	14,37
Lithium	38,28	14,35
Sodium	36,98	13,87
Molten salt	36,92	13,84
Air	36,02	13,51
Neon	35,86	13,45
Sodium-Potassium	35,62	13,36

As the results show, the thermal power absorbed by the fluid varies with the type of fluid used in the central receivers.

5. CONCLUSIONS

The central receiver is an important component of the solar power tower systems. Because the radiation from the heliostats is absorbed directly by the heat transfer fluid of the receiver. In this study, a Solar Two central receiver for model validation is modelled. Later on, different gas and liquid metals were made in ANSYS Fluent, the temperature changes on the receiver and the receiver thermal efficiency were obtained and discussed.

According to the results obtained, the efficiency of the receiver varies between 84,54% and 90,98%. The highest thermal efficiency was obtained from Helium and the lowest thermal efficiency was obtained from the Sodium-Potassium eutectic. Although Helium provided the highest thermal energy efficiency, when it is evaluated in terms of the energy quality depending on the outlet temperature, Sodium-Potassium eutectic liquid metal had the highest exergetic efficiency. On the other hand, Sodium-Potassium's contribution to the reduction in CO_2 emissions is minimal.

Commercially, molten salt is commonly used in solar power tower applications. It was seen that the exergetic efficiency and CO_2 emission decrease values obtained from the analyses conducted in this study supported this situation.

For future work, the corrosion effects and their degradation times can be studied. The economic and availability of these fluids can also be in consideration.

Nomenclature

amb Ambient
ex Exergy
ms Molten salt
rec Receiver
s Sun
th Thermal

c_i CO_2 emission amount of fuel per energy ($kgCO_2/kWh$)

c_p Specific heat of the heat transfer fluid (J/kgK)

$\dot{m}$ Mass flow rate of the heat transfer fluid (kg/s)

$\dot{m}_{CO_2}$ Mass flow rate of CO_2 emission per hour ($kgCO_2/h$)

Q_{abs} Power absorbed by the heat transfer fluid (W)

Q_{loss} Total losses from the receiver (W)

$T_{in,htf}$ Inlet temperature of the heat transfer fluid (K)

$T_{out,htf}$ Outlet temperature of the heat transfer fluid (K)

V_{air} Wind velocity (m/s)

Greek Letters

α Receiver solar absorptance

η Efficiency

References

[1] Colomer, G., Chiva, J., Lehmkuhl, O., and Oliva, A., Advanced CFD and HT numerical modeling of solar tower receivers, *Energy Procedia*, 49, 2014, 50-59.

[2] Rodriguez-Sanchez, M. R., Sanchez-Gonzalez, A., Marugan-Cruz, C., and Santana, D., New designs of molten-salt tubular-receiver for solar power tower, Energy Procedia, 49, 2014, 504-513.

[3] Kribus, A., Doron, P., Rubin, R., Karni, J., Reuven, R., Duchan, S., and Taragan, E., A Multistage Solar Receiver: The Route To High Temperature, *Solar Energy*, 67, 1999, 3-11.

[4] Yang, M., Yang, X., and Ding, J., Heat transfer enhancement and performance of the molten salt receiver of a solar power tower, *Applied Energy*, 87, 2010, 2808-2811.

[5] Christian, J. M., and Ho, C. K., CFD Simulation and Heat Loss Analysis of the Solar Two Power Tower Receiver, Proceedings of ASME 2012 6th International Conference on Energy Sustainability & 10th Fuel Cell Science, Engineering and Technology Conference, San Diego, 2012.

[6] Zanino, R., Bonifetto, R., Christian, J. M., Ho, C. K., and Savoldi Richard, L., Effects of RANS-Type turbulence models on the convective heat loss computed by CFD in the solar two power tower, *Energy Procedia*, 49, 2014, 569-578.

[7] Pacio, J., and Wetzel, T., Assessment of liquid metal technology status and research paths for their use as efficient heat transfer fluids in solar central receiver systems, *Solar Energy*, 93, 2013, 11-22.
[8] Boerema, N., Morrison, G., Taylor, R., and Rosengarten, G., Liquid sodium versus Hitec as a heat transfer fluid in solar thermal central receiver systems, *Solar Energy*, 86, 2012, 2293-2305.
[9] Bellos, E., Tzivanidis, C., and Antonopoulos, K. A., A detailed working fluid investigation for solar parabolic trough collectors, *Applied Thermal Engineering*, 114, 2017, 374-386.
[10] Pacheco, J. E., *Final Test and Evaluation Results from the Solar Two Project*, Sandia National Laboratories, 2002.
[11] AlZahrani, A. A., and Dincer, I., Energy and exergy analyses of a parabolic trough solar power plant using carbon dioxide power cycle, *Energy Conveersion and Management*, 158, 2018, 476-488
[12] https://www.eia.gov/tools/faqs/faq.php?id=73&t=11 (Accessed: 13/02/2018)